Carli *et al.* Supplementary Tables and Figures Index

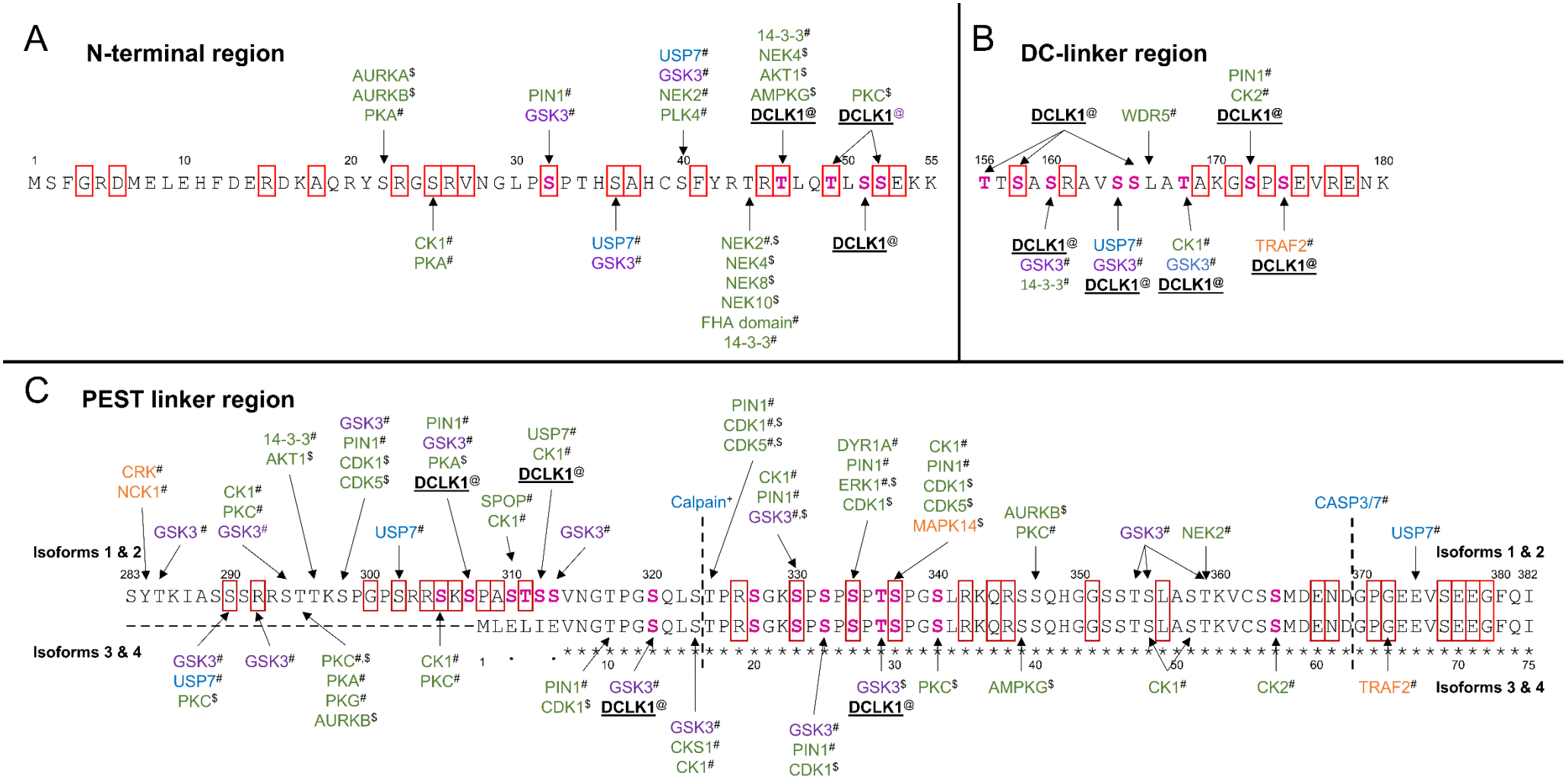

Figure S1. In silico prediction of proteins that interact with the (**A**) N-terminal region, (**B**) DC-linker region, and (**C**) PEST linker region for isoforms 1 & 2 (top) and isoforms 3 & 4 (bottom). Proteins are colored by function: protein degradation (blue), cell cycle processes (green), MAPK cascade (orange), and Wnt signalling (purple). Proteins were identified by Eukaryotic Linear Motif resource (ELM, #) [135], Scansite 4.0 ($) [95], or DeepCalpain (+) software [120], or manually curated from the literature with DCLK1 autophosphorylation sites (@), phosphorylation sites (magenta), and identified mutations (red boxes) from supplementary Table S2.

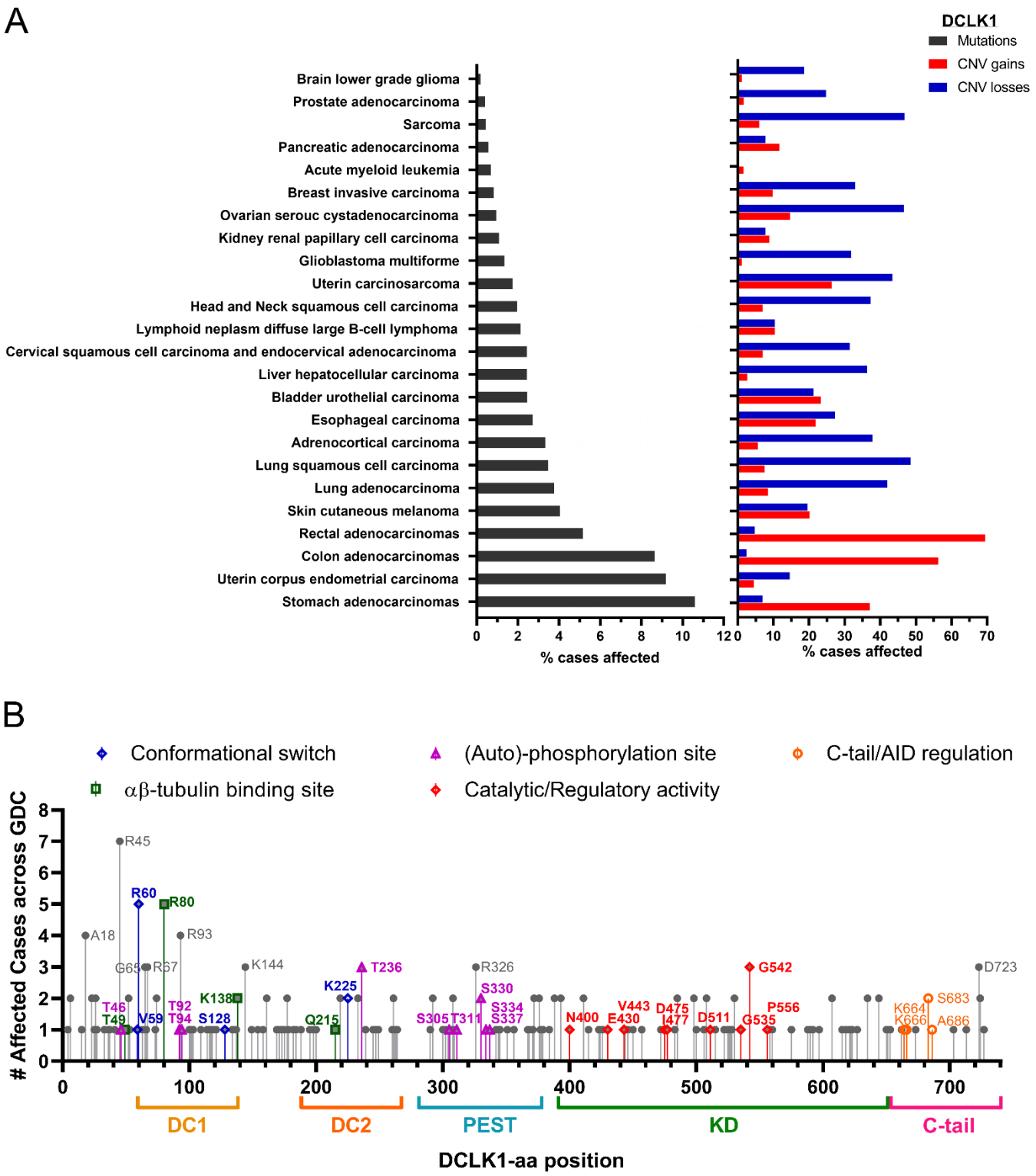

Figure S2 DCLK1 missense mutations in cancer. (**A**) The distribution of the 394 DCLK1 mutations and copy number variation (CNV) gains and losses identified in the genomic data commons (GDC) data-set for each malignancy. (**B**) Lollipop figure showing frequency and position of the DCLK1 missense mutations identified within the GDC cohort. Residues are only labelled if they coincide with a known functional residue, or with ≥ 3 incidences. With residues highlighted involved in the confirmational switch (blue), αβ-tubulin isomeric binding (green), (auto)-phosphorylation (purple), catalytic/regulatory kinase activity motif (red), and C-regulatory tail/auto-inhibitory domain (AID) (orange).

Table S1. Experimentally determined structures of the DC1 and DC2 domains from DCX and DCLK1, and the DCLK1 kinase domain.

Domain	Year	ID	Method	Res.	Protein-Isoform	Conformation	Notes	Reference
DC1	2020	6REV	Cryo-EM	3.8 Å	DCX	C-tail disordered	Cryo-EM structure bound to 13-protofilament GDP-microtubule	[73]
DC1	2020	6RFD	Cryo-EM	3.9 Å	DCX	C-tail disordered	Cryo-EM structure bound to 14-protofilament GDP-microtubule	[73]
DC1	2020	6RF8	Cryo-EM	3.8 Å	DCX	C-tail disordered	Cryo-EM structure bound to 13-protofilament GDP-microtubule	[136]
DC1	2016	5IKC	X-ray	2.06 Å	DCX	C-tail disordered	In complex with Fab 1/108	[75]
DC1	2016	5IN7	X-ray	2.48 Å	DCX	Closed	K215D/K216D mutant	[75]
DC1	2016	5IOI	X-ray	2.4 Å	DCX	Closed (chains C/F) Open (chains A/E) C-tail disordered (chains B/D)	K215D/K216D mutant	[75]
DC1	2016	5IO9	X-ray	1.3 Å	DCX	Closed	K215D/K216D mutant	[75]
DC1	2006	2BQQ	X-ray	2.2 Å	DCX	Open	K215D/K216D mutant	[85]
DC1	2003	1UF0	NMR		DCLK1	Closed		Unpublished
DC1	2003	1MG4	X-ray	1.504 Å	DCLK1	Closed	Unlabelled protein.	[80]
DC1	2003	1MFW	X-ray	1.6 Å	DCLK1	Closed	Selenomethionine labelled protein	[80]
DC1	2003	1MJD	NMR		DCX	Closed		[80]
DC2	2020	6RF2	Cryo-EM	4.2 Å	DCX	Monomeric	Cryo-EM structure bound to microtubules	[73]
DC2	2018	6FNZ	X-ray	2.23 Å	DCX	Domain-swapped dimer	Domain swapped dimer	[86]
DC2	2016	5IP4	X-ray	1.81 Å	DCX	Monomeric	In complex with nanobody XA4451. Closed conformation	[75]
KD	2021	7KX8	X-ray	3.1 Å	DCLK1-1/3 Residues 372-686	Active (Type 1)	DCLK1-Cter in complex with FMF-03-055-1	[54]
KD	2021	7KXW	X-ray	3.002 Å	DCLK1-1/2/3/4 Residues 372-649	Active (Type 1.5)	DCLK1-KD in complex with DCLK1-IN-1	[54]
KD	2021	7KX6	X-ray	2.5 Å	DCLK1-1/2/3/4 Residues 372-649	Active (Type 1)	DCLK1-KD in complex with XMD8-85	[54]
KD	2021	7F3G	X-ray	2.1 Å	DCLK1-1/2/3/4 Residues 372-649	Active (Type 1)	DCLK1 kinase domain in complex with ruxolitinib	[137]
KD	2021	6KYQ	X-ray	2.141 Å	DCLK1-2/4 Residues 379-703	Autoinhibited	DCLK1 Autoinhibited Kinase Domain	[51]
KD	2021	6KYR	X-ray	2.206 Å	DCLK1-2/4 Residues 379-703	Autoinhibited	DCLK1 mutant (P675L) Autoinhibited Kinase Domain	[51]
Domain	**Year**	**ID**	**Method**	**Res.**	**Protein-Isoform**	**Conformation**	**Notes**	**Reference**
KD	2016	5JZJ	X-ray	1.71 Å	DCLK1-1/2/3/4 Residues 372-649	Active (Type 1)	DCLK1-KD in complex with AMPPN	[53]
KD	2016	5JZN	X-ray	2.85 Å	DCLK1-1/2/3/4 Residues 372-649	Active (Type 1)	DCLK1-KD in complex with NVP-TAE684	[53]

Table S2. Functional residues of DCLK1 and their mutation frequency. The proposed function(s) for each identified site in DCX and matched or identified site in DCLK1 are given, including: its mutation frequency according to NCI's GDC portal [115], the amino acid substitutions observed; and the domain in DCLK1 in which it is located. The identified function of the residue which is color coded according to Figure 4 with (auto)phosphorylation sites (magenta), isomeric MT binding sites (green), conformational switch (blue), catalytic/regulatory kinase activity (other colors).

Identified DCX residue	Identified or matched DCLK1 residue	Mutation frequency	Substitution	Domain	Function	Reference
S28	S32				phosphorylation related actin/microtubule binding switch on DCX	[70]
					phosphorylated by CDK5 on DCX	[89]
	T46	1	T>M		(Auto)phosphorylation site identified in mass spectrometry based experiment	[52,53,83]
Q44	Q48				isomeric binding site of DC1 domain (of DCX) to αβ-tubulin	[73]
A45	T49	1	T>M	DC1	isomeric binding site of DC1 domain (of DCX) to αβ-tubulin	[73]
					(Auto)phosphorylation site identified in mass spectrometry based experiment	[83,52]
S47	S51			DC1	phospho-site identified with mass spectrometry based (altered upon C-tail deletion or T668A mutation)	[52]
					Phosphorylated by PKA and MARK on DCX	[20]
					Facilitates Kinesin-3 motor binding along microtubules	[74]
	S52	2	S>Y/C	DC1	Autophosphorylation site identified in mass spectrometry based experiment	[83]
A52	A56			DC1	isomeric binding site of DC1 domain (of DCX) to αβ-tubulin	[73]
K54	K58			DC1	Isomeric binding site of tryptophan -> open DC state	[75,85,80]
V55	V59	1	V>A	DC1	Isomeric binding site of tryptophan -> open DC state	[75,85,80]
R56	R60	5	R>C	DC1	Isomeric binding site of tryptophan -> open DC state	[75,85,80]
	S77			DC1	Phospho-site identified with mass spectrometry based (altered upon C-tail deletion or T668A mutation)	[52]
					DCLK1 phospho-site identified in mass spectrometry based experiment	[49]
R76	R80	5	R>W 3x R>Q 2x	DC1	Isomeric binding site of DC1 domain (of DCX) to αβ-tubulin	[73]
R78	R82			DC1	Isomeric binding site of DC1 domain (of DCX) to αβ-tubulin	[73]
	S83			DC1	phospho-site identified with mass spectrometry based (altered upon C-tail deletion or T668A mutation)	[52]
D81	E85			DC1	Isomeric binding site of DC1 domain (of DCX) to αβ-tubulin	[73]
	T92	1	T>P	DC1	Autophosphorylation site identified in mass spectrometry based experiment	[52]
	T94	1	T>P	DC1	Autophosphorylation site identified in mass spectrometry based experiment	[52]

Identified DCX residue	Identified or matched DCLK1 residue	Mutation frequency	Substitution	Domain	Function	Reference
	S96			DC1	Phospho-site identified with mass spectrometry based (altered upon C-tail deletion or T668A mutation)	[52]
					Autophosphorylation site identified in mass spectrometry based experiment	[83]
N94	N98			DC1	Isomeric binding site of DC1 domain (of DCX) to αβ-tubulin	[73]
R102	R106			DC1	Isomeric binding site of DC1 domain (of DCX) to αβ-tubulin	[73]
	T107			DC1	Autophosphorylation site identified in mass spectrometry based experiment	[52]
	S119			DC1	phospho-site identified with mass spectrometry based (altered upon C-tail deletion or T668A mutation)	[52]
G122	G126			DC1	Isomeric binding site of tryptophan -> open DC state	[75,85,80]
E123	E127			DC1	Isomeric binding site of tryptophan -> open DC state	[75,85,80]
S124	S128	1	S>R	DC1	Isomeric binding site of tryptophan -> open DC state	[75,85,80]
				DC1	Phospho-site identified with mass spectrometry based (altered upon C-tail deletion or T668A mutation)	[52]
K134	K138	2	K>N	DC1	Isomeric binding site of DC1 domain (of DCX) to αβ-tubulin	[73]
	T143				Phospho-site identified with mass spectrometry based (altered upon C-tail deletion or T668A mutation)	[52]
W146	W150				Tryptophan responsible for the open/close confirmation of DC domains	[75,85,80]
	S151				Autophosphorylation site identified in mass spectrometry based experiment	[13,17,18]
	T156				Autophosphorylation site identified in mass spectrometry based experiment	[18]
	S158	1	S>W		Autophosphorylation site identified in mass spectrometry based experiment	[18]
	S160				Autophosphorylation site identified in mass spectrometry based experiment	[53,83,52]
	S164				Autophosphorylation site identified in mass spectrometry based experiment	[53,83,52]
	S165				Autophosphorylation site identified in mass spectrometry based experiment	[83]
	T168				Autophosphorylation site identified in mass spectrometry based experiment	[52]
	S172				Autophosphorylation site identified in mass spectrometry based experiment	[83]
	S174				Autophosphorylation site identified in mass spectrometry based experiment	[83]
	T189			DC2	Phospho-site identified with mass spectrometry based (altered upon C-tail deletion or T668A mutation)	[52]
	S193			DC2	Phospho-site identified with mass spectrometry based (altered upon C-tail deletion or T668A mutation)	[52]
N200	N206			DC2	Isomeric binding site of DC2 domains (of DCX) to αβ-tubulin	[73]
T203	T209			DC2	Isomeric binding site of DC2 domains (of DCX) to αβ-tubulin	[73]
H205	H211			DC2	Isomeric binding site of DC2 domains (of DCX) to αβ-tubulin	[73]

Identified DCX residue	Identified or matched DCLK1 residue	Mutation frequency	Substitution	Domain	Function	Reference
E208	E214			DC2	Isomeric binding site of DC2 domains (of DCX) to αβ-tubulin	[73]
Q209	Q215	1	Q>K	DC2	Isomeric binding site of DC2 domains (of DCX) to αβ-tubulin	[73]
	T218			DC2	Phospho-site identified with mass spectrometry based (altered upon C-tail deletion or T668A mutation)	[52]
K219	K225	1	K>T		KLET/KLDS hinge	[86]
L220	L226				KLET/KLDS hinge	[86]
E221	D227				KLET/KLDS hinge	[86]
T222	S228			DC2	KLET/KLDS hinge	[86]
					Isomeric binding site of DC2 domains (of DCX) to αβ-tubulin	[73]
					Phospho-site identified with mass spectrometry based (altered upon C-tail deletion or T668A mutation)	[52]
V224	V230			DC2	Isomeric binding site of DC2 domains (of DCX) to αβ-tubulin	[73]
	T236	3	T>A 1x T>M 2x	DC2	Autophosphorylation site identified in mass spectrometry based experiment * Full length specific	[52]
	S274			PEST	Autophosphorylation site identified in mass spectrometry based experiment	[53,83]
S297	S298			PEST	Phospho-DCX by CDK5	[18]
	S305	1	S>G	PEST	DCLK1 phospho-site identified in mass spectrometry based experiment	[49]
	S307	1		PEST	DCLK1 phospho-site identified in mass spectrometry based experiment	[49]
					Autophosphorylation site identified in mass spectrometry based experiment	[53]
	T310			PEST	DCLK1 phospho-site identified in mass spectrometry based experiment	[49]
	T311	1	T>I	PEST	DCLK1 phospho-site identified in mass spectrometry based experiment	[49]
	S312			PEST	Autophosphorylation site identified in mass spectrometry based experiment	[53]
	S313			PEST	DCLK1 phospho-site identified in mass spectrometry based experiment	[49]
					Autophosphorylation site identified in mass spectrometry based experiment	[53]
	S320			PEST	Autophosphorylation site identified in mass spectrometry based experiment	[53]
T321	T324			PEST	Phospho-DCX by JNK	[105]
	S327			PEST	DCLK1 phospho-site identified in mass spectrometry based experiment	[49]
S332	S330	2	S>L	PEST	Phospho-DCX by JNK	[107]
					DCLK1 phospho-site identified in mass spectrometry based experiment	[49]
	S332			PEST	DCLK1 phospho-site identified in mass spectrometry based experiment	[49,48]
T331	S334	1	S>L	PEST	Phospho-DCX by JNK	[105]
					DCLK1 phospho-site identified in mass spectrometry based experiment	[49]

Identified DCX residue	Identified or matched DCLK1 residue	Mutation frequency	Substitution	Domain	Function	Reference
	T336			PEST	DCLK1 phospho-site identified in mass spectrometry based experiment	[49,48]
					Autophosphorylation site identified in mass spectrometry based experiment	[53]
S334	S337	1	S>N	PEST	Phospho-DCX by JNK	[105]
					DCLK1 phospho-site identified in mass spectrometry based experiment	[49,48]
	S340			PEST	DCLK1 phospho-site identified in mass spectrometry based experiment	[49]
	S364				DCLK1 phospho-site identified in mass spectrometry based experiment	[48]
	T395			KD	Autophosphorylation site identified in mass spectrometry based experiment	[83]
	N400	1	N>H	KD	Part of Glycine rich loop	[53]
	V404			KD	Critical residue in C-spine / ATP binding	[53]
	A417			KD	Critical residue in C-spine	[53]
	K419			KD	ATP binding	[53]
	E430	1	E>K	KD	Part of αC-helix	[53]
	E436			KD	ATP binding	[53]
	S438			KD	Autophosphorylation site identified in mass spectrometry based experiment	[83]
	L440			KD	Critical residue in R-spine	[53]
	V443	1	V>L	KD	Part of αC-helix	[53]
	L451			KD	Critical residue in R-spine	[53]
	L473			KD	Critical residue in C-spine	[53]
	D475	1	D>N	KD	Involved in hinge region with AID domain	[51]
	I477	1	I>T	KD	Involved in hinge region with AID domain	[51]
	M491			KD	Critical residue in C-spine	[53]
	H509			KD	HRD motif / Critical residue in R-spine	[53]
	R510			KD	HRD motif	[53]
	D511	1	D>N	KD	HRD motif / D511N is kinase dead mutant	[53]
	L517			KD	Critical residue in C-spine	[53]
	V519			KD	Critical residue in C-spine	[53]
	D533			KD	DFG motif	[53]
	F534			KD	DFG motif / Critical residue in R-spine	[53]
	G535	1	G>E	KD	DFG motif	[53]
	G542	3	G>V 1x	KD	part of the activation loop	[53]
			G>D 2x			
	T546			KD	Conserved phosphorylation-site in activation loop	[53]
	P556	1	P>A	KD	Part of the activation loop	[53]

Identified DCX residue	Identified or matched DCLK1 residue	Mutation frequency	Substitution	Domain	Function	Reference
	D569			KD	Critical residue in R-spine	[53]
	I576			KD	Critical residue in C-spine	[53]
	L580			KD	Critical residue in C-spine	[53]
	S637			KD	Autophosphorylation site identified in mass spectrometry based experiment	[53]
	V661			C-tail	Hydrophobic interaction of R1 with KD	[51]
	K664	1	K>N	C-tail	Part of R1 helix	[51]
	I665			C-tail	Hydrophobic interaction of R1 with KD	[51]
	K666	1	K>N	C-tail	Part of R1 helix	[51]
	T668			C-tail	Autophosphorylation-site for AID domain regulation	[52]
	F669			C-tail	Hydrophobic interaction of R1 with KD	[51]
	T678*			C-tail	Autophosphorylation site identified in mass spectrometry based experiment	[53]
	V682			C-tail	Hydrophobic interaction of R2 with KD	[51]
	S683	2	S>Y	C-tail	Part of R2 helix	[51]
	V684			C-tail	Hydrophobic interaction of R2 with KD	[51]
	I685			C-tail	Hydrophobic interaction of R2 with KD	[51]
	A686	1	A>T	C-tail	Part of R2 helix	[51]
	K692			C-tail	Key residue of R3 that forms salt bridges with D511 and D533	[51]
	T692*			C-tail	Autophosphorylation site identified in mass spectrometry based experiment	[53]
	R698			C-tail	Hydrophilic interaction with KD	[51]
	R701			C-tail	Hydrophilic interaction with KD	[51]
	S720			C-tail	DCLK1 phospho-site identified in mass spectrometry based experiment	[48]
	S726			C-tail	DCLK1 phospho-site identified in mass spectrometry based experiment	[48]

Table S3. Predicted impact of point mutations on the structural stability of DCLK1. Predictions were performed using the DynaMut2 server [138] on mutations for which an experimental structure was available (either of DCX or DCLK1). The impact on stability was classified according to the change in Gibbs Free Energy ($\Delta\Delta G^{Stability}$): neutral ($-0.5 < \Delta\Delta G^{Stability} < 0.5$ kcal/mol), mildly destabilising ($0.5 \leq \Delta\Delta G^{Stability} < 1$ kcal/mol), or destabilising ($\Delta\Delta G^{Stability} \geq 1$ kcal/mol).

Mutation	**Domain**	**PDB ID (Protein)**	**Predicted stability change ($\Delta\Delta G^{Stability}$) in kcal/mol**	**Predicted Impact**
T49M	N-terminal region	6REV (DCX-Tubulin, A45M)	-0.7	Mildly destabilising
V59A	DC1	1MG4 (DCLK1)	-2.41	Destabilising
R60C	DC1	1MG4 (DCLK1)	-1.78	Destabilising
G65A	DC1	6REV (DCX-Tubulin, G61A)	-0.21	Neutral
G65R	DC1	6REV (DCX-Tubulin, G61R)	-0.62	Mildly destabilising
R67G	DC1	1MG4 (DCLK1)	-0.49	Mildly destabilising
R67Q	DC1	1MG4 (DCLK1)	-0.38	Neutral
R80Q	DC1	6REV (DCX-Tubulin, R76Q)	-0.54	Mildly destabilising
R80W	DC1	6REV (DCX-Tubulin, R76W)	-1.02	Destabilising
T92P	DC1	6REV (DCX-Tubulin, T88P)	-0.39	Neutral
R93Q	DC1	6REV (DCX-Tubulin, R89N)	-0.54	Mildly destabilising
T94P	DC1	6REV (DCX-Tubulin, S90P)	-0.44	Neutral
S128R	DC1	1MG4 (DCLK1)	0.42	Neutral
K138N	DC1	6REV (DCX-Tubulin, K134N)	-0.31	Neutral
K144N	DC1	1MG4 (DCLK1)	0.43	Neutral
K144R	DC1	1MG4 (DCLK1)	0.1	Neutral
Q215K	DC2	6RF2 (DCX-Tubulin, Q209K)	0.23	Neutral
K225R	DC2	6RF2 (DCX-Tubulin, K219R)	-0.07	Neutral
K225T	DC2	6RF2 (DCX-Tubulin, K219R)	-0.38	Neutral
T236A	DC2	5IP4 (DCX, T230A)	-0.81	Mildly destabilising
T236M	DC2	5IP4 (DCX, T230M)	0.1	Neutral
N400H	Kinase domain	5JZJ (DCLK1)	-0.07	Neutral
E430K	Kinase domain	5JZJ (DCLK1)	0.31	Neutral
V443L	Kinase domain	5JZJ (DCLK1)	-0.5	Mildly destabilising
D475N	Kinase domain	5JZJ (DCLK1)	0.05	Neutral
I477T	Kinase domain	5JZJ (DCLK1)	-2.82	Destabilising
D511N	Kinase domain	5JZJ (DCLK1)	-0.37	Neutral
G535E	Kinase domain	5JZJ (DCLK1)	-1.68	Destabilising
G542D	Kinase domain	5JZJ (DCLK1)	-0.27	Neutral
G542V	Kinase domain	5JZJ (DCLK1)	-1.33	Destabilising
P556A	Kinase domain	5JZJ (DCLK1)	-1.08	Destabilising
K664N	C-tail	6KYQ (DCLK1)	-1.54	Destabilising
K666N	C-tail	6KYQ (DCLK1)	-0.08	Neutral
P673H	C-tail	6KYQ (DCLK1)	-0.11	Neutral
S683Y	C-tail	6KYQ (DCLK1)	-0.99	Destabilising
A686T	C-tail	6KYQ (DCLK1)	-0.78	Mildly destabilising

References

18. Tanaka, T.; Serneo, F.F.; Tseng, H.C.; Kulkarni, A.B.; Tsai, L.H.; Gleeson, J.G. Cdk5 Phosphorylation of Doublecortin Ser297 Regulates Its Effect on Neuronal Migration. *Neuron* **2004**, *41*, 215–227. https://doi.org/10.1016/S0896-6273(03)00852-3.
20. Schaar, B.T.; Kinoshita, K.; McConnell, S.K. Doublecortin Microtubule Affinity Is Regulated by a Balance of Kinase and Phosphatase Activity at the Leading Edge of Migrating Neurons. *Neuron* **2004**, *41*, 203–213. https://doi.org/10.1016/s0896-6273(03)00843-2.
48. Ferguson, F.M.; Nabet, B.; Raghavan, S.; Liu, Y.; Leggett, A.L.; Kuljanin, M.; Kalekar, R.L.; Yang, A.; He, S.; Wang, J.; et al. Discovery of a Selective Inhibitor of Doublecortin like Kinase 1. *Nat. Chem. Biol.* **2020**, *16*, 635–643. https://doi.org/10.1038/s41589-020-0506-0.
49. Liu, Y.; Ferguson, F.M.; Li, L.; Kuljanin, M.; Mills, C.E.; Subramanian, K.; Harshbarger, W.; Gondi, S.; Wang, J.; Sorger, P.K.; et al. Chemical Biology Toolkit for DCLK1 Reveals Connection to RNA Processing. *Cell Chem. Biol.* **2020**, *27*, 1229–1240.e4. https://doi.org/10.1016/j.chembiol.2020.07.011.
51. Cheng, L.; Yang, Z.; Guo, W.; Wu, C.; Liang, S.; Tong, A.; Cao, Z.; Thorne, R.F.; Yang, S.-Y.; Yu, Y.; et al. DCLK1 Autoinhibition and Activation in Tumorigenesis. *Innovation* **2022**, *3*, 100191. https://doi.org/10.1016/j.xinn.2021.100191.
52. Agulto, R.L.; Rogers, M.M.; Tan, T.C.; Ramkumar, A.; Downing, A.M.; Bodin, H.; Castro, J.; Nowakowski, D.W.; Ori-McKenney, K.M. Autoregulatory Control of Microtubule Binding in Doublecortin-like Kinase 1. *eLife* **2021**, *10*, e60126. https://doi.org/10.7554/eLife.60126.
53. Patel, O.; Dai, W.; Mentzel, M.; Griffin, M.D.W.; Serindoux, J.; Gay, Y.; Fischer, S.; Sterle, S.; Kropp, A.; Burns, C.J.; et al. Biochemical and Structural Insights into Doublecortin-like Kinase Domain 1. *Structure* **2016**, *24*, 1550–1531. https://doi.org/10.1016/j.str.2016.07.008.
54. Patel, O.; Roy, M.J.; Kropp, A.; Hardy, J.M.; Dai, W.; Lucet, I.S. Structural Basis for Small Molecule Targeting of Doublecortin Like Kinase 1 with DCLK1-IN-1. *Commun. Biol.* **2021**, *4*, 1105. https://doi.org/10.1038/s42003-021-02631-y.
70. Moslehi, M.; Ng, D.C.H.; Bogoyevitch, M.A. Doublecortin X (DCX) Serine 28 Phosphorylation Is a Regulatory Switch, Modulating Association of DCX with Microtubules and Actin Filaments. *Biochim. Biophys. Acta—Mol. Cell Res.* **2019**, *1866*, 638–649. https://doi.org/10.1016/j.bbamcr.2019.01.003.
73. Manka, S.W.; Moores, C.A. Pseudo-repeats in Doublecortin Make Distinct Mechanistic Contributions to Microtubule Regulation. *EMBO Rep.* **2020**, *21*, e51534. https://doi.org/10.15252/embr.202051534.
74. Liu, J.S.; Schubert, C.R.; Fu, X.; Fourniol, F.J.; Jaiswal, J.K.; Houdusse, A.; Stultz, C.M.; Moores, C.A.; Walsh, C.A. Molecular Basis for Specific Regulation of Neuronal Kinesin-3 Motors by Doublecortin Family Proteins. *Mol. Cell* **2012**, *47*, 707–721. https://doi.org/10.1016/j.molcel.2012.06.025.
75. Burger, D.; Stihle, M.; Sharma, A.; Di Lello, P.; Benz, J.; D'Arcy, B.; Debulpaep, M.; Fry, D.; Huber, W.; Kremer, T.; et al. Crystal Structures of the Human Doublecortin C- and N-Terminal Domains in Complex with Specific Antibodies. *J. Biol. Chem.* **2016**, *291*, 16292–16306, doi:10.1074/jbc.M116.726547.
80. Kim, M.H.; Cierpicki, T.; Derewenda, U.; Krowarsch, D.; Feng, Y.; Devedjiev, Y.; Dauter, Z.; Walsh, C.A.; Otlewski, J.; Bushweller, J.H.; et al. The DCX-Domain Tandems of Doublecortin and Doublecortin-like Kinase. *Nat. Struct. Biol.* **2003**, *10*, 324–333. https://doi.org/10.1038/nsb918.
83. Sugiyama, N.; Imamura, H.; Ishihama, Y. Large-Scale Discovery of Substrates of the Human Kinome. *Sci. Rep.* **2019**, *9*, 10503. https://doi.org/10.1038/s41598-019-46385-4.
85. Cierpicki, T.; Kim, M.H.; Cooper, D.R.; Derewenda, U.; Bushweller, J.H.; Derewenda, Z.S. The DC-Module of Doublecortin: Dynamics, Domain Boundaries, and Functional Implications. *Proteins Struct. Funct. Bioinform.* **2006**, *64*, 874–882. https://doi.org/10.1002/prot.21068.
86. Rufer, A.C.; Kusznir, E.; Burger, D.; Stihle, M.; Ruf, A.; Rudolph, M.G. Domain Swap in the C-Terminal Ubiquitin-like Domain of Human Doublecortin. *Acta Crystallogr. Sect. D Struct. Biol.* **2018**, *74*, 450–462. https://doi.org/10.1107/S2059798318004813.
89. Graham, M.E.; Ruma-Haynes, P.; Capes-Davis, A.G.; Dunn, J.M.; Tan, T.C.; Valova, V.A.; Robinson, P.J.; Jeffrey, P.L. Multisite Phosphorylation of Doublecortin by Cyclin-Dependent Kinase 5. *Biochem. J.* **2004**, *381*, 471–481. https://doi.org/10.1042/BJ20040324.
95. Obenauer, J.C.; Cantley, L.C.; Yaffe, M.B. Scansite 2.0: Proteome-Wide Prediction of Cell Signaling Interactions Using Short Sequence Motifs. *Nucleic Acids Res.* **2003**, *31*, 3635–3641. https://doi.org/10.1093/nar/gkg584.
105. Gdalyahu, A.; Ghosh, I.; Levy, T.; Sapir, T.; Sapoznik, S.; Fishler, Y.; Azoulai, D.; Reiner, O. DCX, a New Mediator of the JNK Pathway. *EMBO J.* **2004**, *23*, 823–832. https://doi.org/10.1038/sj.emboj.7600079.
107. Jin, J.; Suzuki, H.; Hirai, S.; Mikoshiba, K.; Ohshima, T. JNK Phosphorylates Ser332 of Doublecortin and Regulates Its Function in Neurite Extension and Neuronal Migration. *Dev. Neurobiol.* **2010**, *70*, 929–942. https://doi.org/10.1002/dneu.20833.
115. Grossman, R.L.; Heath, A.P.; Ferretti, V.; Varmus, H.E.; Lowy, D.R.; Kibbe, W.A.; Staudt, L.M. Toward a Shared Vision for Cancer Genomic Data. *N. Engl. J. Med.* **2016**, *375*, 1109–1112. https://doi.org/10.1056/NEJMp1607591.
120. Liu, Z.-X.; Yu, K.; Dong, J.; Zhao, L.; Liu, Z.; Zhang, Q.; Li, S.; Du, Y.; Cheng, H. Precise Prediction of Calpain Cleavage Sites and Their Aberrance Caused by Mutations in Cancer. *Front. Genet.* **2019**, *10*, 715. https://doi.org/10.3389/fgene.2019.00715.
135. Kumar, M.; Michael, S.; Alvarado-Valverde, J.; Mészáros, B.; Sámano-Sánchez, H.; Zeke, A.; Dobson, L.; Lazar, T.; Örd, M.; Nagpal, A.; et al. The Eukaryotic Linear Motif Resource: 2022 Release. *Nucleic Acids Res.* **2022**, *50*, D497–D508, doi:10.1093/nar/gkab975.
136. Cook, A.D.; Manka, S.W.; Wang, S.; Moores, C.A.; Atherton, J. A Microtubule RELION-Based Pipeline for Cryo-EM Image Processing. *J. Struct. Biol.* **2020**, *209*, 107402, doi:10.1016/j.jsb.2019.10.004.
137. Jang, D.M.; Lim, H.J.; Hahn, H.; Lee, Y.; Kim, H.K.; Kim, H.S. Structural Basis of Inhibition of DCLK1 by Ruxolitinib. *Int. J. Mol. Sci.* **2021**, *22*, 8488, doi:10.3390/ijms22168488.
138. Rodrigues, C.H.M.; Pires, D.E.V.; Ascher, D.B. DynaMut2: Assessing Changes in Stability and Flexibility upon Single and Multiple Point Missense Mutations. *Protein Sci.* **2021**, *30*, 60–69, doi:10.1002/pro.3942.